Available online at www.sciencedirect.com

SciVerse ScienceDirect

Ceramics International 38 (2012) 3607–3612

CERAMICS INTERNATIONAL

www.elsevier.com/locate/ceramint

Phase structure and thermophysical properties of co-doped $La_2Zr_2O_7$ ceramics for thermal barrier coatings

Jianying Xiang, Shuhai Chen, Jihua Huang *, Hua Zhang, Xingke Zhao

School of Materials Science and Engineering, University of Science and Technology Beijing, Beijing 100083, China

Received 13 December 2011; received in revised form 28 December 2011; accepted 29 December 2011
Available online 8 January 2012

Abstract

$La_2Zr_2O_7$ has high melting point, low thermal conductivity and relatively high thermal expansion which make it suitable for application as high-temperature thermal barrier coatings. Ceramics including $La_2Zr_2O_7$, $(La_{0.7}Yb_{0.3})_2(Zr_{0.7}Ce_{0.3})_2O_7$ and $(La_{0.2}Yb_{0.8})_2(Zr_{0.7}Ce_{0.3})_2O_7$ were synthesized by solid state reaction. The effects of co-doping on the phase structure and thermophysical properties of $La_2Zr_2O_7$ were investigated. The phase structures of these ceramics were identified by X-ray diffraction, showing that the $La_2Zr_2O_7$ ceramic has a pyrochlore structure while the co-doped ceramics $(La_{0.7}Yb_{0.3})_2(Zr_{0.7}Ce_{0.3})_2O_7$ and the $(La_{0.2}Yb_{0.8})_2(Zr_{0.7}Ce_{0.3})_2O_7$ exhibit a defect fluorite structure, which is mainly determined by ionic radius ratio $r(A_{av.}^{3+})/r(B_{av.}^{4+})$. The measurements for thermal expansion coefficient and thermal conductivity of these ceramics from ambient temperature to 1200 °C show that the co-doped ceramics $(La_{0.7}Yb_{0.3})_2(Zr_{0.7}Ce_{0.3})_2O_7$ and $(La_{0.2}Yb_{0.8})_2(Zr_{0.7}Ce_{0.3})_2O_7$ have a larger thermal expansion coefficient and a lower thermal conductivity than $La_2Zr_2O_7$, and the $(La_{0.2}Yb_{0.8})_2(Zr_{0.7}Ce_{0.3})_2O_7$ shows the more excellent thermophysical properties than $(La_{0.7}Yb_{0.3})_2(Zr_{0.7}Ce_{0.3})_2O_7$ due to the increase of Yb_2O_3 content.

Keywords: Thermal conductivity; Thermal expansion; Ceramic; Co-doping

1. Introduction

Thermal barrier coatings (TBCs) are widely used in turbine engines to protect hot-section metallic components from corrosion and oxidation [1,2]. The conventional TBCs material in commercial use is stabilized zirconia with 8 wt.% yttria (8YSZ). However, it could hardly be used for long-term application at temperatures above 1200 °C due to its low sintering resistance and low phase structure stability, which increases thermal conductivity and makes them less effective [3,4]. In the next generation of advanced engines, further increase in thrust-to-weight ratio will require even higher gas turbine inlet temperature. So it is urgently needed to develop new TBCs materials with a significantly lower thermal conductivity and better sintering resistance than 8YSZ [5]. However, the selection of TBCs materials is restricted by some basic requirements such as high melting point, low thermal conductivity, high thermal expansion coefficient, high phase stability, and low sintering rate [6,7]. It is found by many researchers [8–10] that the rare earth zirconates show promising thermophysical properties. Its general composition is $A_2B_2O_7$, where A is a 3^+ cation (La to Lu) and B is a 4^+ cation (Zr, Ce, Hf, etc.), such as $La_2Zr_2O_7$, it has excellent thermal stability, low sintering rate and low thermal conductivity. However, its thermal expansion is low compare to 8YSZ ($9.1 \times 10^{-6}\ K^{-1}$ at 1000 °C for $La_2Zr_2O_7$ and $10.1 \times 10^{-6}\ K^{-1}$ at 1000 °C for 8YSZ) [11–13].

In recent studies, it has been reported that materials with lower thermal conductivity and higher thermal expansion coefficient can be prepared by doping or co-doping with one or more oxides (Yb_2O_3, CeO_2, Gd_2O_3, Sm_2O_3, and Nd_2O_3) due to defect cluster formation, which indicates that the thermal conductivity of $La_2Zr_2O_7$ may be reduced further by doping with other elements in the cation of La or Zr [14,15]. Clarke and coworkers [16] also points out that substituted cation, especially the atom with large atomic weight, at site A or B creates mass disorder on the cation sublattice, which results in the lowering of thermal conductivity. Meanwhile the thermal expansion coefficient is proved to be higher by Cao et al. [17].

The primary objective of the present work was to devise approaches to further lower the thermal conductivity and higher

---

* Corresponding author. Tel.: +86 10 62334859; fax: +86 10 62334859.
E-mail address: jihuahuang47@sina.com (J. Huang).

0272-8842/$36.00 © 2012 Elsevier Ltd and Techna Group S.r.l. All rights reserved.
doi:10.1016/j.ceramint.2011.12.077

the thermal expansion coefficient of $La_2Zr_2O_7$. Oxides co-doping approach was used where part of cations A and B were substituted by other elements in $La_2Zr_2O_7$ ceramic. The $La_2Zr_2O_7$, $(La_{0.7}Yb_{0.3})_2(Zr_{0.7}Ce_{0.3})_2O_7$ and $(La_{0.2}Yb_{0.8})_2(Zr_{0.7}Ce_{0.3})_2O_7$ ceramics were synthesized by solid state reaction. Their thermal conductivities and thermal expansion coefficients were measured, and the effects of co-doping on the phase structure and thermophysical properties were also investigated.

2. Experiment

In the present study, ZrO_2 (Shanghai St-Nano Science and Technology Co. Ltd., purity ≥99.99%), La_2O_3, Yb_2O_3 and CeO_2 (GRIPM Advanced Materials Co. Ltd., purity ≥99.99%) were chosen as the reactants. The oxide powders were fired at 900 °C for 5 h before weighing. After mixed the stoichiometric constituents of $La_2Zr_2O_7$, $(La_{0.7}Yb_{0.3})_2(Zr_{0.7}Ce_{0.3})_2O_7$ and $(La_{0.2}Yb_{0.8})_2(Zr_{0.7}Ce_{0.3})_2O_7$ by ball milling in analytically pure alcohol and dried at 110 °C for 6 h in vacuum drying oven, these ceramics were synthesized by solid state reaction at 1600 °C for 12 h.

For thermal conductivity measurements, these ceramics powder were uniaxially hot-pressed into disk-shaped samples with $\Phi 12.7 \times (2\text{–}3)$ mm using a 12.7 mm diameter graphite die at 1600 °C and 45 MPa pressure for 4 h. The hot-pressed pellets were heat treated for 6 h at 800 °C in air for oxidation of the surface carbon layer deposited on the samples during hot pressing.

The phase structure of each ceramic was characterized by X-ray diffraction (XRD, Rigaku D/Max 2500, Japan) with Ni filtered Cu Kα radiation (0.1542 nm) at the scanning rate of 4°/min. The microstructure of the pellets was examined using field emission scanning electron microscopy (FESEM, ZEISS ULTRA55). The bulk densities (ρ) of hot-pressed pellets were measured by the Archimedes principle with an immersion medium of deionized water.

The specific heat capacities (C_p) of these ceramics were measured using differential scanning calorimetry (DSC, Netzsch DSC204-F1, Germany) in the range of ambient temperature to 1200 °C. The thermal expansion coefficients of these ceramics were determined with a high-temperature dilatometer (Netzsch DIL402C/7, Germany) from ambient temperature to 1200 °C at a heating rate of 5 °C/min in argon atmosphere. The size of samples is approximately $\Phi 10 \times 6$ mm. The hot-pressed pellets of three ceramics were used for thermal diffusivity (λ) measurements. Thermal diffusivity testing of the ceramic discs was carried out using laser-flash method on the laser flash apparatus (Netzsch LFA427, Germany) in an argon atmosphere. Before measurements, both the front and back faces of these samples were coated with a thin layer of colloidal graphite. These coatings were done to prevent direct transmission of laser beam through the translucent specimen at high temperatures. Each specimen was measured three times at room temperature, 200 °C, 400 °C, 600 °C, 800 °C, 1000 °C and 1200 °C.

The thermal conductivities (k) of the samples were calculated by the following equation with specific heat capacity (C_p), density (ρ) and thermal diffusivity (λ):

$$\kappa = \lambda \cdot \rho \cdot C_p \tag{1}$$

Because the sintered samples were not fully dense (100%), the measured values of thermal conductivity were modified for the actual value k_0 using the following Eq. (2), where φ is the fractional porosity [18].

$$\frac{k}{k_0} = 1 - \frac{4}{3}\varphi \tag{2}$$

3. Results and discussion

3.1. Microstructure and relative density

The typical microstructure of $(La_{0.7}Yb_{0.3})_2(Zr_{0.7}Ce_{0.3})_2O_7$ and $(La_{0.2}Yb_{0.8})_2(Zr_{0.7}Ce_{0.3})_2O_7$ ceramics is shown in Fig. 1. The interfaces between grains are very clean, the gap is very small and no other interphases and unreacted oxides existed in boundaries between grains. Fig. 2 shows the relative density of $La_2Zr_2O_7$, $(La_{0.7}Yb_{0.3})_2(Zr_{0.7}Ce_{0.3})_2O_7$ and $(La_{0.2}Yb_{0.8})_2(Zr_{0.7}Ce_{0.3})_2O_7$ ceramics sintered at 1600 °C and 45 MPa pressure for 4 h. Each specimen has a high relative density due to the high temperature and high pressure in the hot pressing process.

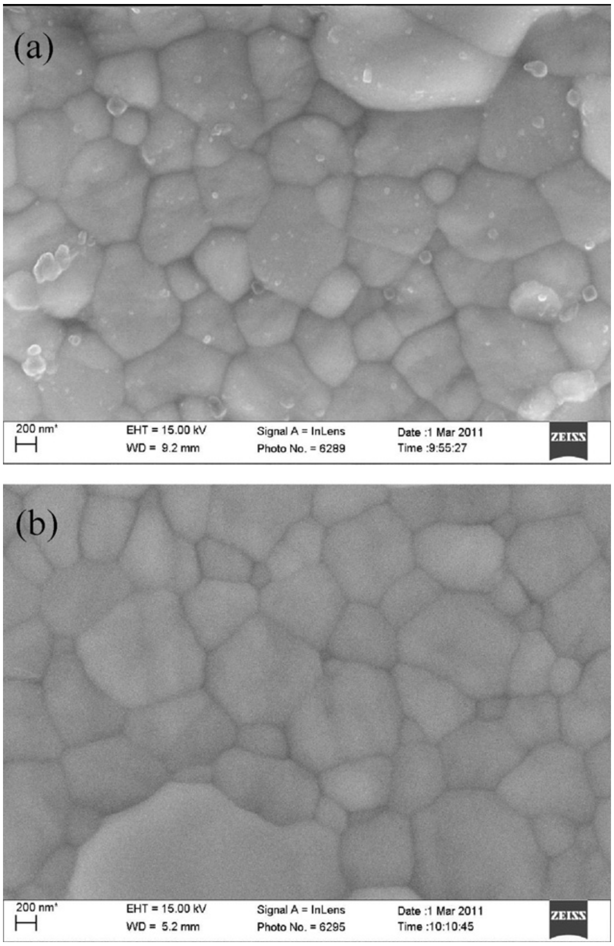

Fig. 1. Typical microstructure of $(La_{0.7}Yb_{0.3})_2(Zr_{0.7}Ce_{0.3})_2O_7$ (a) and $(La_{0.2}Yb_{0.8})_2(Zr_{0.7}Ce_{0.3})_2O_7$ (b) ceramics.